Fast climate impact emulation for global temperature scenarios with the Rapid Impact Model Emulator (RIME)

Edward Byers [1]*, Michaela Werning [1], Mahé Perrette [2], Niklas Schwind [1], Volker Krey [1], Keywan Riahi [1] & Carl-Friedrich Schleussner [1, 3]

[1] Energy, Climate and Environment Program, International Institute for Applied Systems Analysis, Schlossplatz 1, 2361 Laxenburg, Austria
[2] Alfred Wegener Institute, Telegrafenberg A 45, 14473 Potsdam, Germany
[3] IRI THESys, Humboldt-Universität zu Berlin, Unter den Linden 6, 10099 Berlin, Germany

* Corresponding author: byers@iiasa.ac.at

Peer review status:
This is a non-peer-reviewed preprint submitted to EarthArXiv.

Abstract

Climate model emulation has long been applied to assess the global climate outcomes of IAM emissions scenarios, but is typically limited to first-order climate variables like mean surface air temperatures at minimal regional resolution. Here we introduce RIME, the Rapid Impact Model Emulator, which uses global warming level interpolation approaches based on inputs of global mean air temperature pathways to calculate a range of climate impacts and exposure indicators in gridded spatial and region-aggregated formats. The emulation is fast and versatile, moving towards batches of climate impact indicators to complement integrated assessment model scenarios thereby bridging the IPCC WGII and WGIII communities. Our lightweight emulator produces both gridded and regionally-aggregated results taking us beyond the constraints of super-computational global climate and impact models. The approach allows to assess the combined outcome of a wide range of emission and socio-economic scenarios allowing for a decomposition of drivers of uncertainty for future climate risks. While climate uncertainties are the primary concern through mid-century, our results indicates that socio-economic factors such population growth may become the dominant drivers of risk by the end of the century. We demonstrate an application to IPCC scenarios to illustrate potential further use, illustrating its potential utility while acknowledging methodological constraints and delineating a comprehensive roadmap for future development. These rapid climate risk emulation frameworks exhibit significant promise for facilitating cross-disciplinary integration and enhancing scientific inclusivity across diverse research communities.

1 Introduction

Climate models in their simplest forms represent the basic energy balance between incoming and outgoing solar radiation and the earth's atmosphere. State of the art, complex earth system models (ESMs) represent the earth's atmosphere, land surface, oceans, cryosphere, carbon and bio-geochemical cycles in spatially gridded forms, simulations of which need to be run on supercomputers and can take weeks to months to complete. ESMs are typically constrained to running in the order of tens of scenarios as part of highly structured, community-driven model intercomparison exercises, such as the Coupled Model Intercomparison Project (CMIP), a process which from initial scenario design to complete assessment in IPCC Working Group 1 (WGI) (Masson-Delmotte et al., 2021), typically takes over five to seven years. Yet, there is a demand for a more agile exploration of climate impacts for different emission scenarios. In response, a class of simple climate models (SCMs) focusing on representing global climate outcomes such as global mean surface temperature (GMT) have emerged. Examples of such SCMs, or reduced-complexity climate models (RCMs), include FAiR (Smith et al., 2018), MAGICC (Meinshausen et al., 2011), OSCAR (Gasser et al., 2017; Quilcaille et al., 2023a), HECTOR (Hartin et al., 2015) and CICERO-SCM (Sandstad et al., 2024). Some of these were evaluated in IPCC WGI in the Reduced Complexity Model Intercomparison Project (RCMIP - Nicholls et al., 2020), as well as IPCC WGIII (Riahi et al., 2022) in the climate assessment (Kikstra et al., 2022) of the mitigation scenarios database (Byers et al., 2022).

Global SCMs allow efficient exploration of radiative forcing or emissions scenarios along many dimensions, be it long-duration simulations, many varied emissions pathways and or in probabilistic modes sampling parametric uncertainties.

Simple climate models allow for a computationally efficient assessment of global warming outcomes for a wide range of emission pathways. Assessing global warming outcomes is directly relevant for global climate policy, but requires translation into regional climate (impact) outcomes. A fundamental insight from the latest

IPCC AR6 is that a wide range of climate (impact) indicators scale well with global mean temperature increase. This allows to derive regional and spatially-explicit responses as a function of global warming levels. One approach of doing so is pattern scaling (Frieler et al., 2012) that typically assumes linear relationships between the local variables and changes in global mean temperature. It works best with temperature, whilst precipitation can be more subject to non-linearities and localized influences from different climate forcers (Myhre et al., 2018). An alternative approach that does not require to assume a functional dependency is time-slicing (James et al., 2017), a method used in climate scenario assessment to make comparison of climate-related (or any) variables, at a given global warming levels, e.g. 1.5, 2 or 3 °C. It derives from the transient climate response to emissions (Allen et al., 2009), and subsequently, a range of other climate impact indicators at global warming levels has been assessed, e.g. (Piontek et al., 2014; Schleussner et al., 2016; Byers et al., 2018, p. 201; Lange et al., 2020; Werning et al., 2024b). The policy-relevance of the approach gained popularity since the Paris Agreement of 2015 and featured in the cross working group Special Report on Global Warming of 1.5°C and in the 6th Assessment Reports of the Intergovernmental Panel on Climate Change (Hoegh-Guldberg et al., 2018; IPCC, 2023). While these approaches can serve the purpose of assessing long-term average climate outcomes, they lack insights on changes in climate variability.

More recently, generative spatially explicit emulator approaches have been developed to reproduce a growing number of climate variables including climate variability. This collection of models has been initially developed with the intention of emulating gridded ESM output and has demonstrated good performance on the CMIP ensemble. STITCHES (Tebaldi et al., 2022) applies primarily a time-slicing approach (James et al., 2017), evaluating the global mean temperature and rate of warming to sample slices from any output variables of an existing ESM output archive. MESMER (Beusch et al., 2020) takes the regional response through global mean temperature pattern scaling while introducing natural variability around the mean response through stochastic processes. Whilst STITCHES can rapidly re-produce multi-variate variables from the ESM output archive, MESMER requires a bespoke calibration process per variable. Initial developments were made for annual (Beusch et al., 2020; Quilcaille et al., 2022) and monthly temperatures (Nath et al., 2022), and it has subsequently been applied to the composite variables of fire weather index and soil moisture (Quilcaille et al., 2023b) and the joint emulation of monthly temperature and precipitation (Schöngart et al., 2024). MERCURY (Nath et al., 2024) extends the MESMER methods in a multi-variate manner using a memory-efficient data compression and lifting scheme, is intended for emulating compound extremes and is demonstrated for the humid-heat metric of wet-bulb globe temperature. Lastly, QuickClim (Kitsios et al., 2023) applies machine learning techniques and is based on CO_2 concentrations, bypasses the need for the GMT trajectory and has been demonstrated for 7 first order ESM variables in a multi-variate setting.

Ultimately, this essentially extends the post-processing chain from integrated assessment model (IAM) emissions scenarios to global mean temperatures, and subsequently to spatial climate variables, enabling the calculation of predefined indicators and extremes. However, the variables currently available from such approaches tend to be first-order climate variable outputs from ESMs like mean air temperatures and precipitation, with much of the development and progress in this field focused on emulating ESM output, for example by introducing annual or monthly natural variability, or by understanding their performance in low emissions scenarios, at varying levels of aerosols or under overshoot conditions (Schwaab et al., 2024). And whilst efforts have been made to extend in the direction of other indicators derived from first order ESM variables, development of new indicators requires substantial research time effort and, without further post-processing, somewhat limits emulators' ability in understanding the socioeconomic risks of climate change in a timely manner.

Here, we demonstrate a workflow to complement IAM scenario research with a broader range of climate impacts information. We use global warming levels which is combined into a workflow and software package called the Rapid Impacts Model Emulator (RIME). RIME takes the GMT pathway, e.g. from an IAM+RCM scenario, combined with an impacts database, to calculate a range of climate impacts and exposure indicators based on the GMT pathway. In this case we use post-processed climate impact variables based on data from the Inter-Sectoral Inter-Model Intercomparison Project (ISIMIP) (Werning et al., 2024b, 2024a), which comprises a suite of ESM and impact model datasets generated using common modelling protocols. The process is designed to be fast and versatile, moving towards batches of climate impact indicators that can be used as both inputs or post-processed outputs of IAM emissions scenarios. The approach and outputs are not intended to be directly comparable, but complementary to the aforementioned ESM emulators. RIME intentionally pushes forwards through the climate impacts chain to produce multiple, independent climate impact and risk indicators for different temperature pathways. Thus, the complexity is currently reduced, for example by not yet including inter-annual variability, for the sake of providing transient indicators of hazard and exposure suitable for integrated assessment modelling (see section 4).

The approach and accompanying software have been designed to work at the interface between the climate impacts and integrated assessment modelling communities, ensuring familiarity with data formats for the users. Within the Intergovernmental Panel for Climate Change (IPCC), this is the interface between working groups II and III, whilst global research communities primarily include the Inter-Sectoral Impacts Modelling Intercomparison Project (ISIMIP (“ISIMIP,” 2024)) and the Integrated Assessment Modelling Consortium (IAMC, (“IAMC,” 2024)). Depending on the inputs available and outputs required, both gridded and table data can be produced. Currently, there are two key applications intended: i) post-processing, such that global integrated assessment model scenarios with temperature pathways can be rapidly complemented by a suite of climate hazard and exposure data to facilitate the comparison of mitigation strategies with incurred impacts; and ii) input-processing, such that with a given IAM scenario of known temperature pathway, climate impact input datasets, for example on air temperatures, water resources and crop yield potentials, can be generated through time to endogenize climate impacts into the IAM for a climate-feedback run.

The rest of this paper describes the methodology, typical workflow and use cases, illustrates the functionality, and concludes with a discussion on limitations and directions for further development.

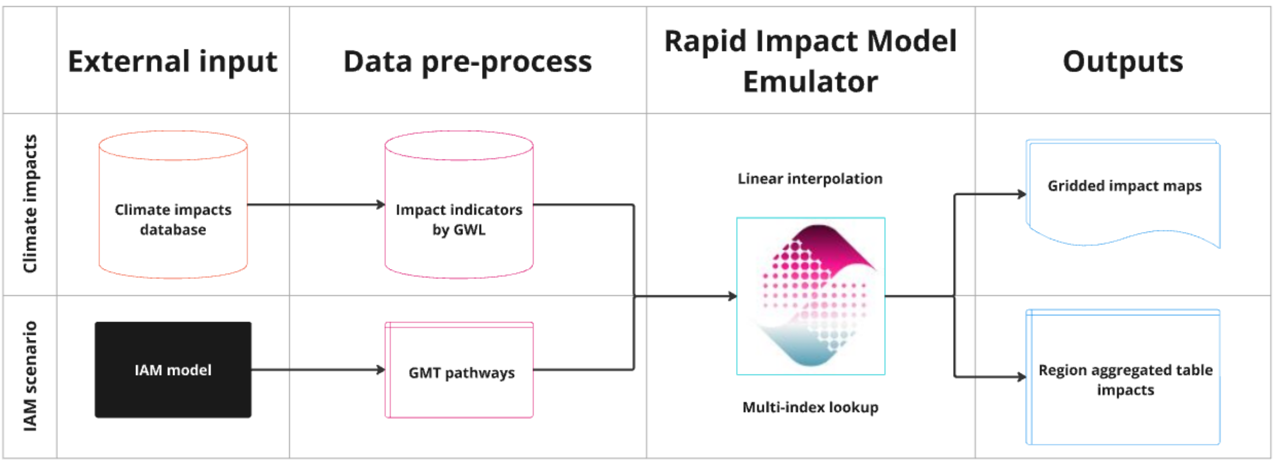

Figure 1. Overview of the general workflow

2 Methodology

2.1 Background

Within RIME, input data is provided at GWLs, obtained through temperature time-slicing, thus providing an empirical map of impact indicators onto GWLs that, unlike normal pattern-scaling (Wells et al., 2023), does not require the assumption of linearity. Only subsequently are intermediate values linearly interpolated, thus essentially a piece-wise pattern-scaling. An assumption or knowledge of an underlying functional form is not required, thereby allowing RIME to be applied with any impact indicator mainly dependent on the global mean temperature level and the provided socioeconomic data.

2.2 Workflow overview

The approach for using RIME requires broadly the following steps:

1. Input pre-processing: a (time-sampled) input database of climate impacts and risk data by global warming levels (GWLs) and socioeconomic scenarios, which can be both gridded and tabular inputs. Default temperature resolution as used here is 0.5 °C, although finer resolution is also possible. Gridded inputs are called raster arrays. Table inputs, which would have values aggregated to a region (e.g. country, IPCC climate zone, etc.), are called region arrays.
2. Linear interpolation: the datasets are linearly interpolated between GWLs to high resolution (e.g. 0.01 or 0.05 °C), whilst other dimensions, which could be non-numeric and categorical, e.g. a socioeconomic dimension (e.g. SSP), can be preserved discreetly. This forms the input database, which depending on the application, can be interpolated for everything a priori albeit with high storage requirements, or on-the-fly when only specific variables are required.
3. Multi-index lookup: taking the GMT timeseries for the input IAM scenario (a GMT pathway), a multi-index lookup for each timestep (year) to identify the closest GWL and (if relevant) socioeconomic scenario, is performed on the input database, to develop a continuous timeseries of climate impacts data consistent with the warming pathway.
4. Post-processing: comprises routines to develop community-relevant data outputs consistent with ISIMIP and IAMC formats.

Parallelization of this workflow, which combines drawing on heavy input datasets with multiple climate indicators with the need to potentially process 10s or even 100s of GMT pathways, is thus necessary and feasible. Within RIME, the current implementation enables parallelized processing in the following modalities (with the possibility of further development extensions):

1. Multi-scenario mode: multiple GMT pathways are input, with one climate indicator processed for all pathways in parallel. For example, for 5 (or 500) IAM scenarios, this mode provides indicators of heatwave exposure for comparison across the GMT pathway ensemble.
2. Multi-indicator mode: in this case, one GMT pathway is processed, with the calculation of multiple climate indicators occurring in parallel. For example, for one IAM scenario, this mode provides datasets with climate indicators on heatwaves, hydrology, precipitation, etc.

The two use cases above can also be combined such that multiple scenarios are processed for multiple indicators, which is implemented by parallelizing the processing of multiple scenarios using the multi-indicator mode (2). In any case, impacts and exposure data for each scenario are subsequently calculated in the order of seconds to minutes on a desktop workstation, depending on the number of indicators and temporal resolution.

To provide a more contextually informative description of the methodology, the sections that follow describe the implementation as tested and described in Table 1 using an impacts dataset (Werning et al., 2024b, 2024a) largely based on ISIMIP3b data.

2.3 Pre-processing the climate impacts input database

A database of post-processed climate impacts (Werning et al., 2024b, 2024a) from global climate CMIP6 & ISIMIP3 ESMs and hydrological impacts models at 0.5° spatial resolution and at GWL intervals from 1.2 (current day) and 1.5-3.5 °C above the pre-industrial control period is used. The gridded maps span a range of indicators covering extremes in precipitation and air temperature, wet-bulb temperature heatwaves, seasonal and inter-annual variability of runoff and discharge, drought and water stress index, and cooling degree days. For each GWL, the indicators are available as absolute values, percentage difference to the reference period (1974-2004), or as a comparable 0-6 impact score. The impact score extends previous approaches (Byers et al., 2018), but takes into account both the absolute value of the indicator and the relative change experienced (Werning et al., 2024b), currently showcased on the ENGAGE project Climate Solutions Explorer (www.climate-solutions-explorer.eu). The indicators are also spatially aggregated to various regional units, including country and IPCC regions, and are available as table data. Population and land area exposure above a threshold value for each indicator through time and aggregated for spatial units e.g., countries and R10 regions, are also available.

Table 1.Overview of the dimensions of climate impacts database used to demonstrate the emulation.

	As tested	**Comments**
Input datasets	Climate hazard, impacts & exposure data by GWLs (Werning et al., 2024a)	Gridded and table data. - 0.5° spatial resolution, global coverage - Table data calculates exposure of land area or population by SSP, also through time and at GWLs, above impact thresholds, following approaches in (Byers et al., 2018; Werning et al., 2024b)
Global Warming Levels (GWLs)	1.2, 1.5, 2.0, 2.5, 3.0, 3.5 °C,	Degrees above the pre-industrial control period as defined by the ISIMIP3 protocol, calculated for 31-year time-slices. More granular GWLs as input data would further reduce uncertainties around non-linear responses between these levels.
Socioeconomic pathways	SSPs 1-5	Applicable when assessing regionally-aggregated indicators relating to population exposure
Population exposure	Gridded SSP population projections	Original gridded downscaled SSP population projections (Jones and O'Neill, 2016; KC and Lutz, 2017), re- scaled to the latest version (KC et

		al., 2024; Werning, 2024) are overlaid with the climate impacts data (Werning et al., 2024b).
Exposure threshold	≥3	Pixels with a score ≥3 are considered exposed to moderate climate impacts as per this method (Werning et al., 2024b, 2024a).
Exposure aggregation spatial units	Countries	For 225 countries and states (Perrette, 2023)
	IPCC climate zone regions	For 44 IPCC regions as used in AR6 (Iturbide et al., 2020)
	R5, R6 or R10 regions	For 5, 6 or 10 common global regions, as used by the IAMC and IPCC (IPCC, 2022)
Spatial aggregation methods	Median, Mean	Median and mean take the value across the pixels, with no weighting.
	Land-area weighted	Land-area weighted mean considers the area per 0.5° pixel on a quadrilinear grid, which reduces pixel areas towards the poles. Static through time.
	Population weighted	Population weighted mean considers the changing spatial and temporal distribution of a population within an aggregation unit.

2.4 Multi-index lookup

Taking a GMT pathway through time, e.g. from 2020 to 2100, each temperature in the timeseries is mapped to the interpolated impact and exposure indicator database using multi-dimensional index look-up, based on indicator, year, GMT, and as relevant the SSP or other dimensions (elaborated in the discussion) (Figure 2). This produces two main output products (**Error! Reference source not found.**, **Error! Reference source not found.**) at 5-year or decadal timesteps, consistent with the GMT pathway of the IAM pathway. The first (**Error! Reference source not found.**, left) is gridded maps of climate impacts through time, provided in a spatially gridded netCDF format at 0.5° resolution, the resolution consistently used by ISIMIP. The second output product (**Error! Reference source not found.**, right) is data tables in the IAMC format, that aggregate impacts exposure by spatial units through time, e.g., sum of population exposed to heat stress for each country in the world. These tabular outputs of indicators can then be easily appended to the IAM output results or used as input data.

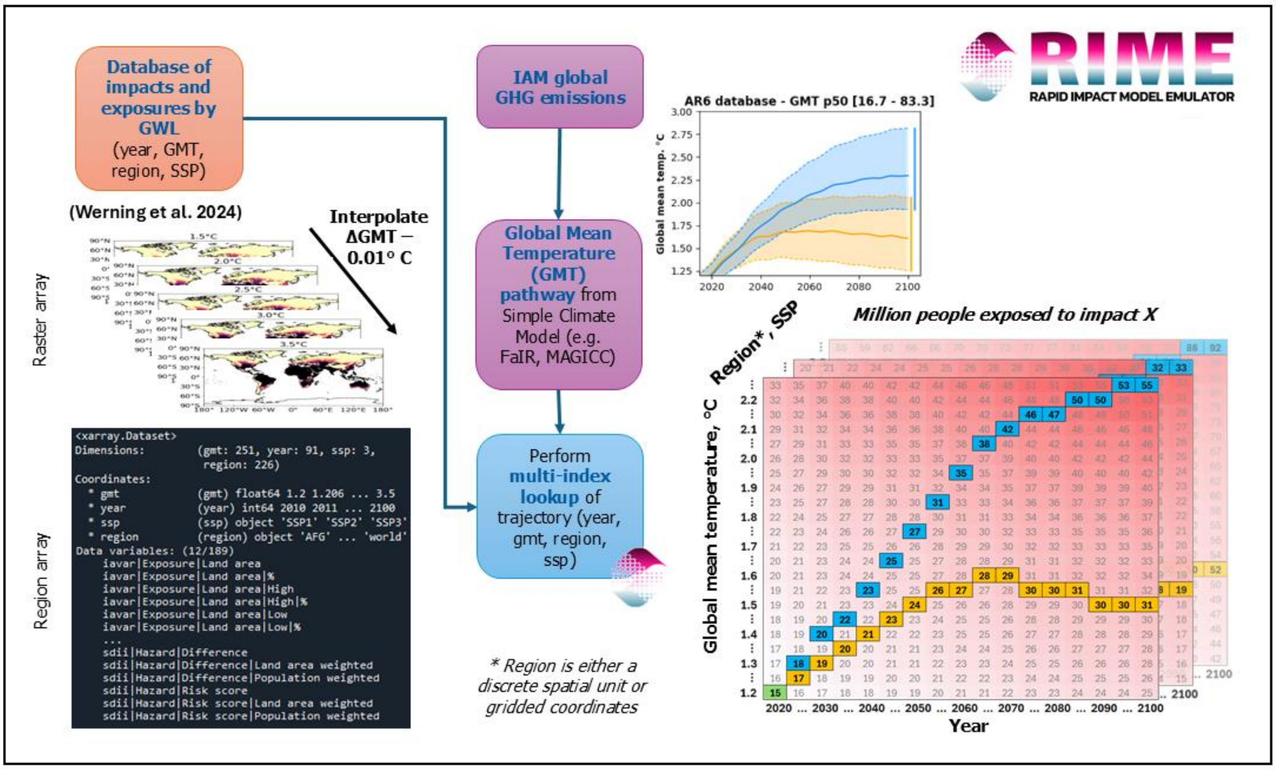

Figure 2. Schematic illustrating the data processing steps. The input datasets (either raster or region array) of impacts and exposure indicators by Global Warming Level are linearly interpolated to a high resolution, and may include other dimensions, e.g., SSP, season, aggregation method. From this the Global Mean Temperature pathway of a global emissions scenario is used in a multi-index lookup to produce the indicator values through time consistent with the GMT pathway of the scenario.

2.5 Implementation

The open-source software is implemented in Python (Rossum and Drake, 2010) and uses, amongst others, the python packages *pyam* (Huppmann et al., 2021) and *pandas* (team, 2024) for table data, *xarray* (Hoyer and Hamman, 2017) for n-dimensional arrays including gridded climate data, and *dask* (Rocklin, 2015) for lazy and parallelized computation. Pyam is a package for analysis, manipulation and visualization of structured data, developed and used by the integrated assessment and energy systems modelling communities. Developed on top of pandas, pyam handles the input and output table-based datasets and ensures conformity and consistency with the IAMC data model. Xarray is used for handling n-dimensional arrays, primarily from the spatially gridded impacts data typically stored in netCDF format and is commonly used in climate research. The climate impacts input database, which could be 10s of GBs in size, also derives from tabular data but is stored as netCDF data and accessed using xarray and dask. Combined with dask, xarray handles the "lazy", as needed reading and computation of such large datasets. Dask is also used explicitly in some of the core functions, to parallelize the processing of either multiple scenarios and indicators.

2.6 Characterization of uncertainty

The default mode of RIME takes a single GMT pathway as input, and provides a corresponding output based on the climate input database. Various use cases for exploring uncertainty are envisaged, however this depends on the input data available, not specifically the emulator (Table 2). In our default use case using the

Werning et al. 2024a datasets, all cases in Table 2 are possible, although the default use case is to use the 50th percentile global mean temperature with multi-model ensemble medians across climate and impact models, with SSP2.

Table 2. Uncertainty categories and examples that can be considered in emulation. This possibility depends however on the input datasets available, not specifically this emulator.

Uncertainty Source	Examples	Description	Available in Werning et al. 2024a
Full range climate model sensitivity (exogenous)	Percentiles, e.g. p5, p17, p25, p33, p50, p67, p75, p83, p95	Full range climate uncertainty, such as from the CMIP6 range assessed by IPCC WGI and used in RCMs like FAiR and MAGICC, can be explored by using GMT pathways at different percentiles as input.	Not applicable
Climate model ensemble members	GFDL-ESM4, IPSL-CM6A-LR, MPI-ESM1-2-HR, ...	Ensemble member uncertainty through comparing results from individual model runs, for example the 5 ESMs used by ISIMIP, or different members from the same ESM.	Yes
Climate forcing scenario	SSP1-26, SSP3-70, SSP5-85	Forcing scenario uncertainty, whereby even for the same ESM and global warming level, different scenarios will have slightly different results.	Yes
Impact model	LPJmL, CLM, CWatM, JULES, ORCHIDEE, …	Multiple impact models, e.g. hydrological or dynamic growth vegetation models, for a given climate will have differences, which is often larger than climate model and forcing uncertainties.	Yes
Socioeconomic scenario	SSP1, SSP2, SSP3,…	Different socioeconomic scenarios may be represented in the impact model, or in exposure and vulnerability calculations. Given its importance in climate impacts and risk assessment, within RIME this is an explicitly coded dimension similar to that of GMT.	Yes

Each indicator and its associated uncertainties will vary by region. It is also possible that some indicators or regions may experience fairly monotonic change with increments of global mean temperature, while for others, there is no clear trend. To evaluate this, the Pearson correlation coefficient between the input GWL data (from 1.2 to 3.5 °C) was calculated for indicators and regions, for the multi-model ensemble median, as well as the 5th and 95th percentiles of the combined climate model and forcing scenario ensemble (Table 3). This feature is included in the software to assist users in evaluating input datasets as to which indicators can be used for which regions. This can be applied to both gridded data and aggregated regions.

Table 3: Trend analysis for the R10 regions and a selection of indicator. A + denotes a positive trend in the data (Pearson coefficient >= 0.8, p value < 0.05), a – denotes a negative trend (Pearson coefficient <= -0.8, p value < 0.05), a . denotes no significant trend. Trends are calculated for the multi-model median (second place) as well as the 5th and 95th

percentile (first and third place, respectively) of the multi-model ensemble; +++ therefore signifies a positive or increasing trend for all three metrics.

Indicator/ Region	Cooling degree days (24 °C)	Heatwave events (5 days, 99th perc.)	Heatwave days (5 days, 99th perc.)	Tropical nights	Consec. dry days	Very heavy precipitation days	Very wet days	Precipitation intensity index
Latin America & Caribbean	+++	+++	+++	+++	+.+	...	+++	.+.
South Asia	+++	+++	+++	+++	-..	..+	+++	..+
Sub-Saharan Africa	+++	+++	+++	+++	...	+.+	.++	+.+
Centrally-planned Asia	+++	+++	+++	+++	---	+++	+++	+++
Middle East	+++	+++	+++	+++	-..	.++	.++	-+.
Eastern and Western Europe	+++	+++	+++	+++	+++	+..	++.	+++
North America	+++	+++	+++	+++	---	+++	+++	+++
Other countries of Asia	+++	+..	+++	+++	...	+.+	+++	+++
Pacific OECD	+++	+++	+++	+++	...	+..	++.	..+
Reforming Economies of Eastern Europe and the Former Soviet Union	+++	+++	+++	+++	---	++.	+++	+++

3 Illustrative results

To illustrate the potential of the emulator, results are presented using two previously unseen emissions scenarios from Working Group III of the IPCC 6th Assessment Report, identified as "Illustrative Pathways". The Moderate Action (ModAct) pathway assumes limited mitigation efforts, exceeding 1.95 °C and 2.69 °C global mean temperature with 50% likelihood in 2050 and 2100, respectively. This is comparable to the 2.7 °C expected under current policies and action by the November 2024 Climate Action Tracker. The Shifting Pathways (SP) scenario is an ambitious mitigation pathway that also assumes substantial progress on the Sustainable Development Goals, reaching 1.51 °C in 2050 and bringing temperatures back down to 1.17 °C by 2100.

Eight climate change indicators from Werning et al. 2024b are chosen for the purpose of projecting climate impacts from these pathways, shown in Figure 3 for 2050 in comparison to simulated 2020. These indicators derive from the temperature and precipitation variables from CMIP6 ESMs, and additionally global hydrological models, and have been published as climate change indicators at global warming levels (Werning et al., 2024b). Thus, the maps presented below are direct representations of the processed indicators (e.g., heatwave events per year, precipitation intensity index), and not post-processed indicators from the underlying temperature and precipitation variables. Further figures for a wider set of temperature, precipitation and hydrological variables are available in the Supporting Information (Figure S 1, Figure S 2).

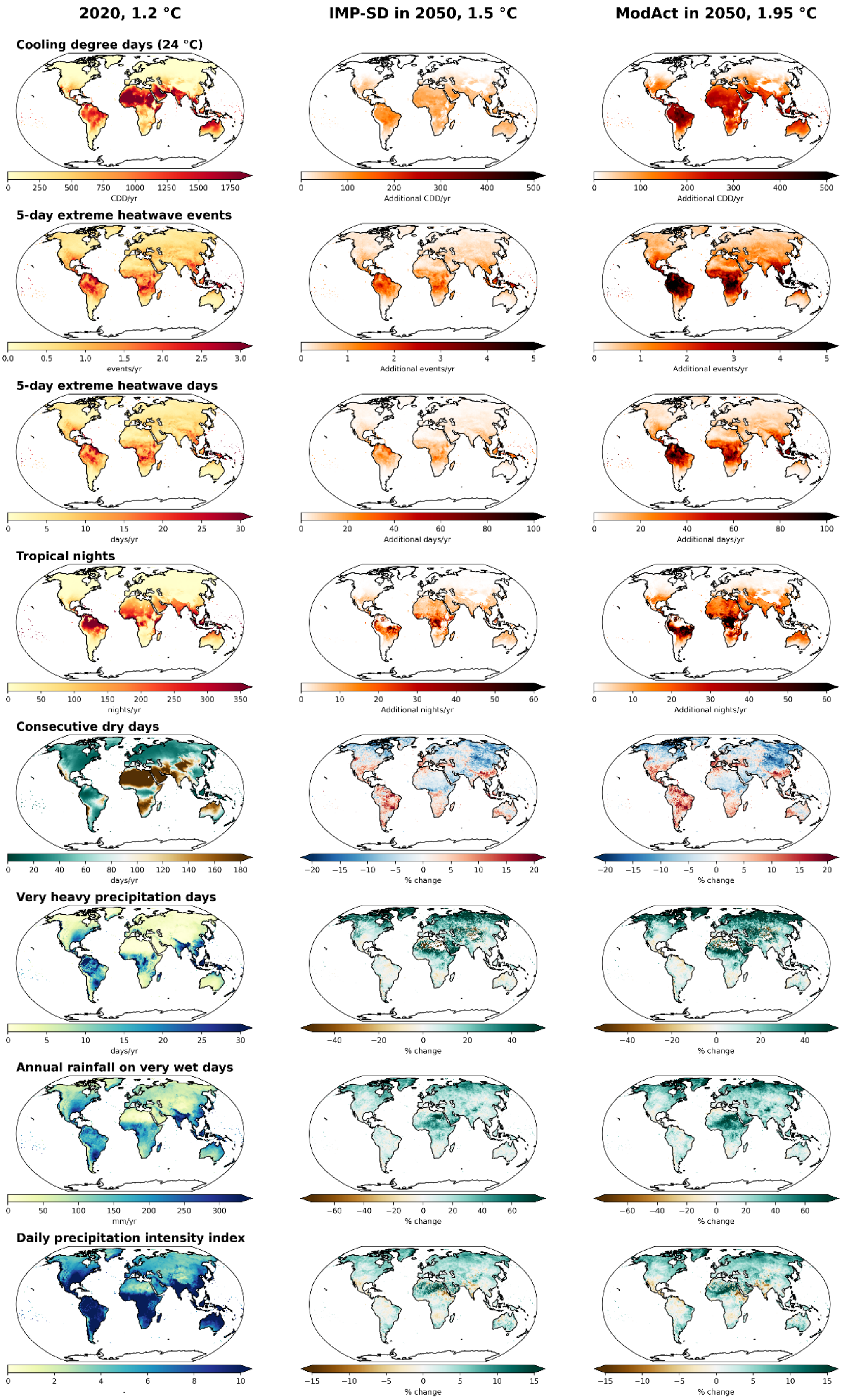

Figure 3. Emulated impact maps for 2020 (left column) and two (unseen) mitigation scenarios in 2050 for 6 selected impact indicators. In the centre and right columns for 2050, the temperature-based indicators are shown as absolute

difference from 2020, whilst the precipitation and hydrological indicators are shown as percentage change. Desert and ice sheet areas are masked out.

Similar results from the same dataset aggregated to regions can be used to explore, for example, population or land area weighted indicators or exposure to these indicators above thresholds (Werning et al., 2024b) (Figure 4). In such cases, the emulation is done directly on the tabular RegionArray data, i.e. where exposure data per region has been aggregated a priori and form part of the input dataset. This could therefore be, for example, by country, climate zones, IPCC or IAM regions - any formulation, even if non-contiguous that can be defined according to the spatial grid.

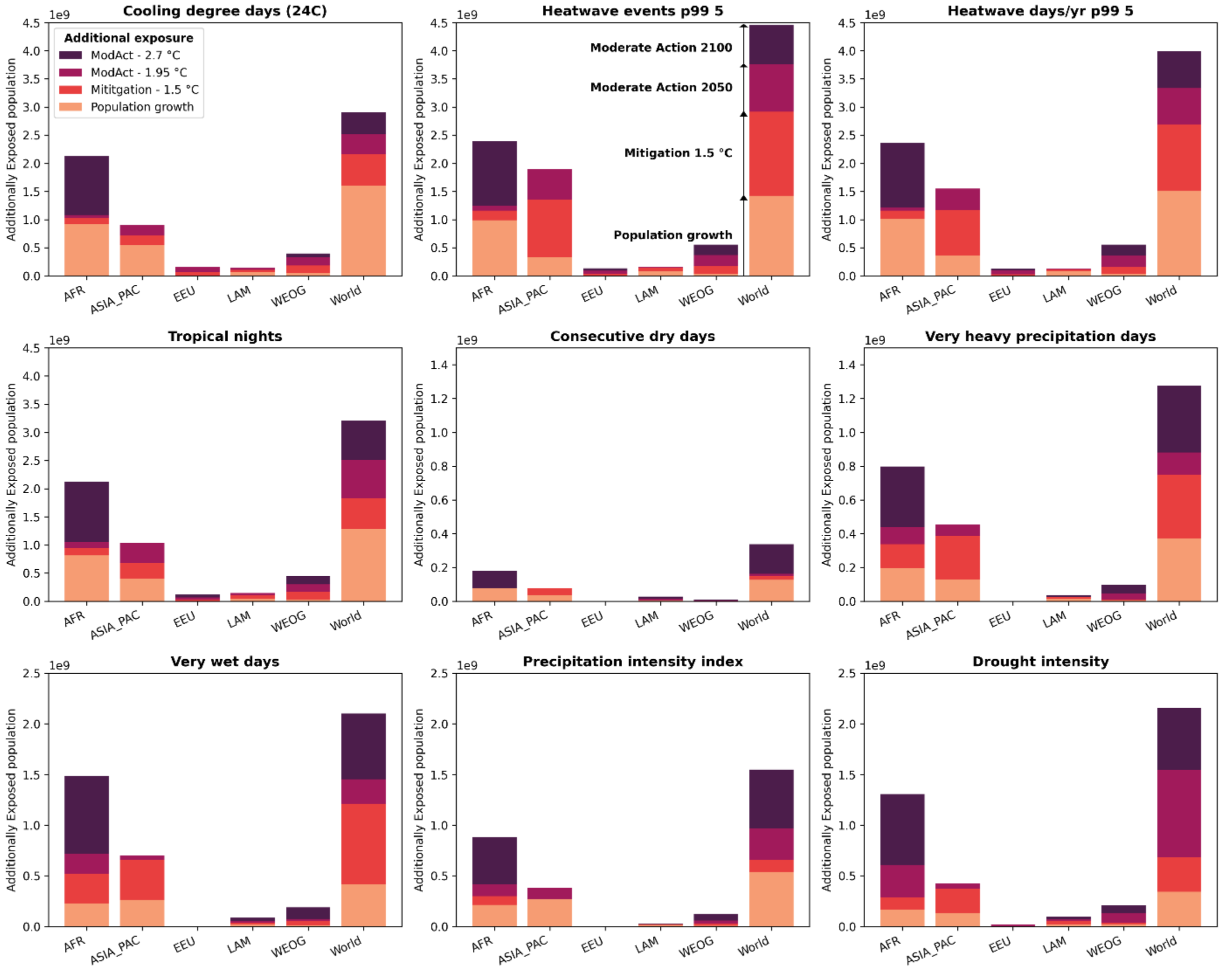

Figure 4. Regionally aggregated results for 5 UN and World regions showing the additional population exposure for nine indictors as driven by population growth (SSP2 in 2050) and climate change, compared to 2020 (1.2 °C). To 2050, population growth in currently exposed regions is substantial, with additional people exposed in the mitigation pathway at 1.5 °C. The Moderate Action pathway exacerbates this further, approximately doubling those exposed compared to mitigation at 1.5 °C in 2050. By 2100 at 2.7 °C the effects are even larger, despite the fact that by this point population in most regions is lower than in 2050. N.B. different y-axis limits.

The additionally exposed population is not only dependent on the different emission scenarios, but also varies with socioeconomic scenario and climate model sensitivity. Figure 5 shows a decomposition of these three different types of uncertainty for a selection of indicators, using the full range of SSPs and a selection of emissions scenarios and MAGICC percentiles. The chosen emissions scenarios include a range of climate categories and IMPs selected for the AR6 of WGIII to span a large range of climate outcomes (Riahi et al., 2022). For the MAGICC percentiles, all percentiles available in the AR6 Scenarios Database are used (Byers et al., 2022) (Table S 4).

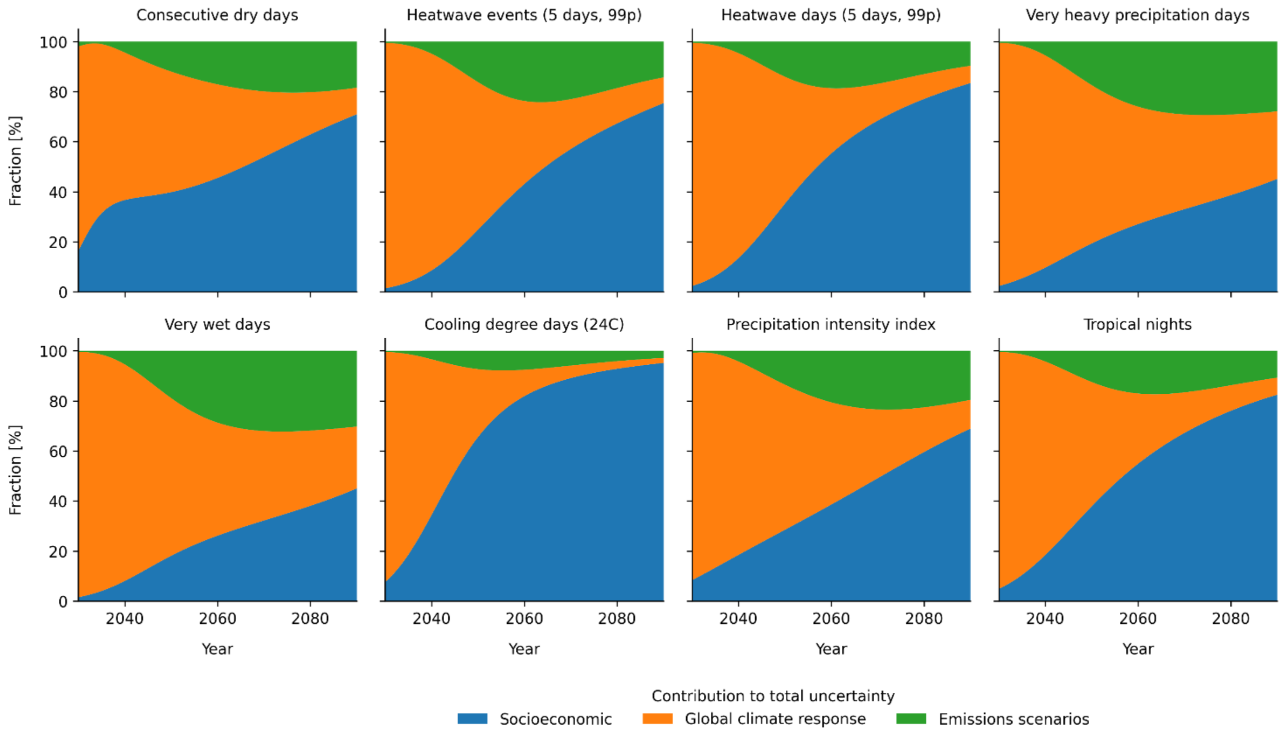

Figure 5: Relative contribution of different sources of uncertainty for the globally exposed population and a selection of indicators.

The relative contribution of the three sources of uncertainty changes throughout the century. While the global climate model sensitivity expressed by the different MAGICC percentiles dominate at the beginning of the century for all indicators, it rapidly declines after the middle of the century, especially for temperature-based indicators. The relative contribution of the socioeconomic scenarios to the total uncertainty shows the opposite trend and steadily increases throughout the century, with a more rapid increase for the temperature-based indicators, and becomes the dominant source of uncertainty by the end of the century. While the relative contribution of the emissions scenarios also increases in the first half of the century, it shows the smallest variation compared to the other two sources and starts to decrease again towards the end of the century. The contributions of the different sources of uncertainty also vary depending on the considered region. For the EU, for example, the uncertainty introduced by the different socioeconomic scenarios still increases with time, but for most indicators stays below 5% (Figure S 6), whereas for Sub-Saharan Africa, it is the dominant factor, contributing to more than 90% of the total uncertainty at the end of the century for temperature-based indicators (Figure S 7). We acknowledge that RIME in its current form does not allow to account for regional climate (impact) uncertainty (Pfleiderer et al., 2025), which is an important area for future development.

4 Discussion and roadmap for development

Based on the current features presented, here we outline some limitations and directions of future development. Broadly, this covers the topics of scenario ensemble assessment, representation of uncertainties and natural variability, overshoot scenarios, input dataset evaluation, and exploration of results.

Approaches to extend uncertainty assessment, including climatic, socioeconomic and scenario based are possible. Exposure and vulnerability scenarios, for example through combining gridded SSP-based data on population (as in (Werning et al., 2024b)) with data on income levels can be used to assess socioeconomic drivers of climate risk. Another area, likely of interest to IPCC WGIII, will be assessing ranges of impacts across mitigation scenario categories, for example by sub-setting ensembles of emissions scenarios by climate categories such as those used in the IPCC WGIII. This will help answer questions like 'How does the range of climate impacts expected by the 97 "1.5 °C (>50%) with no or low overshoot" scenarios (C1) compare to the 311 "likely below (>67%) 2 °C" scenarios (C3)'?

Exploring climate model uncertainties can be currently done in a few ways through controlling the input data (section 2.6, Table 2) and comparison of sources (Figure 5), and will be a focus of further development. Specifically, it is planned to combine climate forcing and climate model uncertainties in a fully probabilistic manner advancing what has been presented here (Table 3, Table S 2, Table S 3) (Schwind, 2025). As shown in Figure 5, in terms of population exposure socioeconomic uncertainty late in the century is substantial particularly in developing regions. Emulation that discerns between different types of forcing scenarios, for example on the level of aerosols, could also be important as pattern scaling has been shown to vary (Goodwin et al., 2020).

The current implementation is not probabilistic and does not attempt to introduce stochastic natural variability, as has been done in other models (e.g. (Beusch et al., 2020; Goodwin et al., 2020; Nath et al., 2022). Although technically possible at annual resolution, it is also important to avoid mis- and over-interpretation of the results whereby users might start to interpret year-to-year variability, hence the default time resolution is 5-year timestep. Furthermore, for typically deterministic IAM scenarios at 5-10 year timesteps, annual variability is not needed and is not consistent with neither input nor output datasets typical of IAMs.

Uncertainties about how climate impacts play out in overshoot pathways means caution is required when assessing impacts post-peak warming (Schleussner et al., 2024). Recent work explored this for regional surface air temperature (Schwaab et al., 2024) using MESMER, but this is less likely to work well for other variables. The default setting in RIME is to not produce results for GMT pathways in years where overshoot temperatures drop more than 0.15 °C below the peak temperature. For a proper overshoot assessment, separate pre- and post-peak temperature impacts databases should be calculated by GWL a priori, such that RIME draws on the relevant impacts database for pre- and post-peak temperature impacts. Simple to implement, there is a lack of overshoot scenario runs from ESM and impacts models available and spanning a number of peak and decline temperature ranges, e.g. peaking at 1.5, 2, 2.5, and 3 °C. Thus, caution is needed with temperature overshoot scenarios or those with high aerosol emissions, where regionalised impacts pre- and post-peak are likely to be different (Shiogama et al., 2023).

The current implementation includes basic diagnostic tools for evaluation of input and output datasets. Determining how the input dataset responds to changes in global warming level at the gridpoint and regional level can be done using the functions demonstrated but could be further advanced both with higher resolution input data and through making statistical comparison to the natural variability of the variable in question. Further checks on input temperature pathway data, for example checking for high levels of aerosol forcing which is a typical output of RCMs, could be used for screening and indicating (low) confidence in regional results.

Lastly, an area of focus will be on further developing user-friendly results dashboards. The current implementation features an interactive HTML dashboard presenting a grid of zoomable and selectable maps, for either a set of scenarios (for one indicator) or a set of indicators (for one scenario). This can be extended to include more user-selectable options such as different timesteps, regionally aggregated plots, distributions, and uncertainty ranges. Further plans also aim to integrate this type of workflow into scenario post-processing routines, such that climate impact indicators of emissions scenarios can be evaluated online on-the-fly, such as online scenario databases like the Scenarios Compass Initiative (https://scenariocompass.org/).

5 Conclusions

Using established global warming level approaches, we demonstrate the rapid post-processing use case allowing ensembles of global IAM mitigation pathways, such as those from the IPCC AR6 scenarios database (Byers et al., 2022), to be accompanied by a new suite of climate impacts and risk information. The initial setup has been designed for proof of concept and is intended to provide indicators of impacts aligned with timeseries of global mean temperatures from IAM scenarios. The approaches are computationally cheap and straightforward to apply, noting that they will not be suitable, in the current form, for certain use cases involving overshoot or impacts with a long memory such as sea-level rise or glacier loss.

Example results using a multi-indicator database are presented for two “Illustrative Pathways” from the IPCC AR6 WGII report. They illustrate use of the RIME software package and estimation of climate impacts for unseen warming trajectories, at gridded and regionally aggregated resolutions. Methods for representing and evaluating regional uncertainties were introduced and explored, with varied success depending on the indicator and region in question. Additional evaluation with more indicators, in particular more from impact models such as for hydrology and crops, will be the focus of further developments in the software.

In summary, it is intended that the software may be used as a post-processing option for IAM scenarios to provide high-level indicators of climate risk and avoided impacts, and thus to better illustrate the benefits of mitigation. The approach bridges a key gap between IPCC WGII and WGIII assessments, connecting the impacts and mitigation communities, respectively, and moves beyond the constraints of RCP pathways enabling a flexible and rapid impacts assessment.

Code & data availability

The RIME package is available under an open-source GPL-3.0 license at https://github.com/iiasa/rime. A Zenodo repository of scripts and data for reproducing the analysis and figures in this manuscript is available at https://doi.org/ 10.5281/zenodo.15049710. This requires the data used from (Werning et al., 2024a) available at https://doi.org/10.5281/zenodo.13753537 .

Acknowledgements

The authors acknowledge funding from the European Union under grant agreements 101081369 (SPARCCLE), 821371 (ENGAGE) for the initial work on the emulator and development of the datasets that underpin the analysis,, and Climate Works Foundation project for Network for Greening the Financial System. Additionally the authors acknowledge the ISIMIP project (www.isimip.org) upon which the data is based.

References:

Allen, M.R., Frame, D.J., Huntingford, C., Jones, C.D., Lowe, J.A., Meinshausen, M., Meinshausen, N., 2009. Warming caused by cumulative carbon emissions towards the trillionth tonne. Nature 458, 1163–1166. https://doi.org/10.1038/nature08019

Beusch, L., Gudmundsson, L., Seneviratne, S.I., 2020. Emulating Earth system model temperatures with MESMER: from global mean temperature trajectories to grid-point-level realizations on land. Earth Syst. Dyn. 11, 139–159. https://doi.org/10.5194/esd-11-139-2020

Byers, E., Gidden, M., Leclere, D., Balkovic, J., Burek, P., Ebi, K., Greve, P., Grey, D., Havlik, P., Hillers, A., Johnson, N., Kahil, T., Krey, V., Langan, S., Nakicenovic, N., Novak, R., Obersteiner, M., Pachauri, S., Palazzo, A., Parkinson, S., Rao, N.D., Rogelj, J., Satoh, Y., Wada, Y., Willaarts, B., Riahi, K., Leclère, D., Balkovic, J., Burek, P., Ebi, K., Greve, P., Grey, D., Havlik, P., Hillers, A., Johnson, N., Kahil, T., Krey, V., Langan, S., Nakicenovic, N., Novak, R., Obersteiner, M., Pachauri, S., Palazzo, A., Parkinson, S., Rao, N.D., Rogelj, J., Satoh, Y., Wada, Y., Willaarts, B., Riahi, K., 2018. Global exposure and vulnerability to multi-sector development and climate change hotspots. Environ. Res. Lett. 13, 055012. https://doi.org/10.1088/1748-9326/aabf45

Byers, E., Krey, V., Kriegler, E., Riahi, K., Schaeffer, R., Kikstra, J., Lamboll, R., Nicholls, Z., Sandstad, M., Smith, C., van der Wijst, K., Lecocq, F., Portugal-Pereira, J., Saheb, Y., Stromann, A., Winkler, H., Auer, C., Brutschin, E., Lepault, C., Müller-Casseres, E., Gidden, M., Huppmann, D., Kolp, P., Marangoni, G., Werning, M., Calvin, K., Guivarch, C., Hasegawa, T., Peters, G., Steinberger, J., Tavoni, M., van Vuuren, D., Al -Khourdajie, A., Forster, P., Lewis, J., Meinshausen, M., Rogelj, J., Samset, B., Skeie, R., 2022. AR6 Scenarios Database. https://doi.org/10.5281/zenodo.7197970

Frieler, K., Meinshausen, M., Mengel, M., Braun, N., Hare, W., 2012. A Scaling Approach to Probabilistic Assessment of Regional Climate Change. https://doi.org/10.1175/JCLI-D-11-00199.1

Gasser, T., Ciais, P., Boucher, O., Quilcaille, Y., Tortora, M., Bopp, L., Hauglustaine, D., 2017. The compact Earth system model OSCAR v2.2: description and first results. Geosci. Model Dev. 10, 271–319. https://doi.org/10.5194/gmd-10-271-2017

Goodwin, P., Leduc, M., Partanen, A.-I., Matthews, H.D., Rogers, A., 2020. A computationally efficient method for probabilistic local warming projections constrained by history matching and pattern scaling, demonstrated by WASP–LGRTC-1.0. Geosci. Model Dev. 13, 5389–5399. https://doi.org/10.5194/gmd-13-5389-2020

Hartin, C.A., Patel, P., Schwarber, A., Link, R.P., Bond-Lamberty, B.P., 2015. A simple object-oriented and open-source model for scientific and policy analyses of the global climate system – Hector v1.0. Geosci. Model Dev. 8, 939–955. https://doi.org/10.5194/gmd-8-939-2015

Hoegh-Guldberg, O., Jacob, D., Taylor, M., 2018. Impacts of 1.5°C of Global Warming on Natural and Human Systems, in: Special Report, Intergovernmental Panel on Climate Change. pp. 175–181.

Hoyer, S., Hamman, J., 2017. xarray: N-D labeled Arrays and Datasets in Python 5, 10. https://doi.org/10.5334/jors.148

Huppmann, D., Gidden, M.J., Nicholls, Z., Hörsch, J., Lamboll, R., Kishimoto, P.N., Burandt, T., Fricko, O., Byers, E., Kikstra, J., Brinkerink, M., Budzinski, M., Maczek, F., Zwickl-Bernhard, S., Welder, L., Álvarez Quispe, E.F., Smith, C.J., 2021. pyam: Analysis and visualisation of integrated assessment and macro-energy scenarios. Open Res. Eur. 1, 74. https://doi.org/10.12688/openreseurope.13633.1

Integrated Assessment Modelling Consortium [WWW Document], 2024. . IAMC. URL https://www.iamconsortium.org/ (accessed 2.25.24).

Inter-Sectoral Impact Model Intercomparison Project [WWW Document], 2024. . ISIMIP. URL https://www.isimip.org/ (accessed 2.25.24).

IPCC, 2023. Climate Change 2023: Synthesis Report. Contribution of Working Groups I, II and III to the Sixth Assessment Report of the Intergovernmental Panel on Climate Change. IPCC, Geneva, Switzerland.

IPCC, 2022. Annex II: Definitions, Units and Conventions, in: Al Khourdaje, A., van Dieman, R., Lamb, W.F., Pathak, M., Reisinger, A., de la Rue du Can, S., Skea, J., Slade, R., Some, S., Steg, L. (Eds.), Climate Change 2022: Mitigation of Climate Change. Contribution of Working Group III to the Sixth Assessment Report of the Intergovernmental Panel on Climate Change. Cambridge University Press, Cambridge, UK and New York, NY, USA, pp. 1821–1840. https://doi.org/10.1017/9781009157926.021

Iturbide, M., Gutiérrez, J.M., Alves, L.M., Bedia, J., Cerezo-Mota, R., Cimadevilla, E., Cofiño, A.S., Di Luca, A., Faria, S.H., Gorodetskaya, I.V., Hauser, M., Herrera, S., Hennessy, K., Hewitt, H.T., Jones, R.G., Krakovska, S., Manzanas, R., Martínez-Castro, D., Narisma, G.T., Nurhati, I.S., Pinto, I., Seneviratne, S.I., van den Hurk, B., Vera, C.S., 2020. An update of IPCC climate reference regions for subcontinental analysis of climate model data: definition and aggregated datasets. Earth Syst. Sci. Data 12, 2959–2970. https://doi.org/10.5194/essd-12-2959-2020

James, R., Washington, R., Schleussner, C.-F., Rogelj, J., Conway, D., 2017. Characterizing half-a-degree difference: a review of methods for identifying regional climate responses to global warming targets. Wiley Interdiscip. Rev. Clim. Change 8, e457-n/a. https://doi.org/10.1002/wcc.457

Jones, B., O'Neill, B.C., 2016. Spatially explicit global population scenarios consistent with the Shared Socioeconomic Pathways. Environ. Res. Lett. 11, 84003. https://doi.org/10.1088/1748-9326/11/8/084003

KC, S., Lutz, W., 2017. The human core of the shared socioeconomic pathways: Population scenarios by age, sex and level of education for all countries to 2100. Glob. Environ. Change 42, 181–192. https://doi.org/10.1016/j.gloenvcha.2014.06.004

KC, S., Moradhvaj, Potancokova, M., Adhikari, S., Yildiz, D., Mamolo, M., Sobotka, T., Zeman, K., Abel, G., Lutz, W., Goujon, A., 2024. Wittgenstein Center (WIC) Population and Human Capital Projections - 2023. https://doi.org/10.5281/zenodo.10618931

Kikstra, J.S., Nicholls, Z.R.J., Smith, C.J., Lewis, J., Lamboll, R.D., Byers, E., Sandstad, M., Meinshausen, M., Gidden, M.J., Rogelj, J., Kriegler, E., Peters, G.P., Fuglestvedt, J.S., Skeie, R.B., Samset, B.H., Wienpahl, L., van Vuuren, D.P., van der Wijst, K.-I., Al Khourdajie, A., Forster, P.M., Reisinger, A., Schaeffer, R., Riahi, K., 2022. The IPCC Sixth Assessment Report WGIII climate assessment of mitigation pathways: from emissions to global temperatures. Geosci. Model Dev. 15, 9075–9109. https://doi.org/10.5194/gmd-15-9075-2022

Kitsios, V., O'Kane, T.J., Newth, D., 2023. A machine learning approach to rapidly project climate responses under a multitude of net-zero emission pathways. Commun. Earth Environ. 4, 1–15. https://doi.org/10.1038/s43247-023-01011-0

Lange, S., Volkholz, J., Geiger, T., Zhao, F., Vega, I., Veldkamp, T., Reyer, C.P.O., Warszawski, L., Huber, V., Jägermeyr, J., Schewe, J., Bresch, D.N., Büchner, M., Chang, J., Ciais, P., Dury, M., Emanuel, K., Folberth, C., Gerten, D., Gosling, S.N., Grillakis, M., Hanasaki, N., Henrot, A.-J., Hickler, T., Honda, Y., Ito, A., Khabarov, N., Koutroulis, A., Liu, W., Müller, C., Nishina, K., Ostberg, S., Müller Schmied, H., Seneviratne, S.I., Stacke, T., Steinkamp, J., Thiery, W., Wada, Y., Willner, S., Yang, H., Yoshikawa, M., Yue, C., Frieler, K., 2020. Projecting Exposure to Extreme Climate Impact Events Across Six Event

Categories and Three Spatial Scales. Earths Future 8, e2020EF001616. https://doi.org/10.1029/2020EF001616

Lehner, F., Deser, C., 2023. Origin, importance, and predictive limits of internal climate variability. Environ. Res. Clim. 2, 023001. https://doi.org/10.1088/2752-5295/accf30

Masson-Delmotte, V., Zhai, P., Pirani, A., Connors, S.L., Péan, C., Berger, S., Caud, N., Chen, Y., Goldfarb, L., Gomis, M.I., others, 2021. Summary for policymakers, in: Climate Change 2021: The Physical Science Basis. Contribution of Working Group I to the Sixth Assessment Report of the Intergovernmental Panel on Climate Change. Cambridge University Press.

Meinshausen, M., Raper, S.C.B., Wigley, T.M.L., 2011. Emulating coupled atmosphere-ocean and carbon cycle models with a simpler model, MAGICC6 – Part 1: Model description and calibration. Atmospheric Chem. Phys. 11, 1417–1456. https://doi.org/10.5194/acp-11-1417-2011

Myhre, G., Kramer, R.J., Smith, C.J., Hodnebrog, Ø., Forster, P., Soden, B.J., Samset, B.H., Stjern, C.W., Andrews, T., Boucher, O., Faluvegi, G., Fläschner, D., Kasoar, M., Kirkevåg, A., Lamarque, J.-F., Olivié, D., Richardson, T., Shindell, D., Stier, P., Takemura, T., Voulgarakis, A., Watson-Parris, D., 2018. Quantifying the Importance of Rapid Adjustments for Global Precipitation Changes. Geophys. Res. Lett. 45, 11,399-11,405. https://doi.org/10.1029/2018GL079474

Nath, S., Carreau, J., Kornhuber, K., Pfleiderer, P., Schleussner, C.-F., Naveau, P., 2024. MERCURY: A fast and versatile multi-resolution based global emulator of compound climate hazards. https://doi.org/10.48550/arXiv.2501.04018

Nath, S., Lejeune, Q., Beusch, L., Seneviratne, S.I., Schleussner, C.-F., 2022. MESMER-M: an Earth system model emulator for spatially resolved monthly temperature. Earth Syst. Dyn. 13, 851–877. https://doi.org/10.5194/esd-13-851-2022

Nicholls, Z.R.J., Meinshausen, M., Lewis, J., Gieseke, R., Dommenget, D., Dorheim, K., Fan, C.-S., Fuglestvedt, J.S., Gasser, T., Golüke, U., Goodwin, P., Hartin, C., Hope, A.P., Kriegler, E., Leach, N.J., Marchegiani, D., McBride, L.A., Quilcaille, Y., Rogelj, J., Salawitch, R.J., Samset, B.H., Sandstad, M., Shiklomanov, A.N., Skeie, R.B., Smith, C.J., Smith, S., Tanaka, K., Tsutsui, J., Xie, Z., 2020. Reduced Complexity Model Intercomparison Project Phase 1: introduction and evaluation of global-mean temperature response. Geosci. Model Dev. 13, 5175–5190. https://doi.org/10.5194/gmd-13-5175-2020

Perrette, M., 2023. ISI-MIP/isipedia-countries (v2.6).

Pfleiderer, P., Frölicher, T.L., Kropf, C.M., Lamboll, R.D., Lejeune, Q., Capela Lourenço, T., Maussion, F., McCaughey, J.W., Quilcaille, Y., Rogelj, J., Sanderson, B., Schuster, L., Sillmann, J., Smith, C., Theokritoff, E., Schleussner, C.-F., 2025. Reversal of the impact chain for actionable climate information. Nat. Geosci. 18, 10–19. https://doi.org/10.1038/s41561-024-01597-w

Piontek, F., Müller, C., Pugh, T.A.M., Clark, D.B., Deryng, D., Elliott, J., De Jesus Colón González, F., Flörke, M., Folberth, C., Franssen, W., Frieler, K., Friend, A.D., Gosling, S.N., Hemming, D., Khabarov, N., Kim, H., Lomas, M.R., Masaki, Y., Mengel, M., Morse, A., Neumann, K., Nishina, K., Ostberg, S., Pavlick, R., Ruane, A.C., Schewe, J., Schmid, E., Stacke, T., Tang, Q., Tessler, Z.D., Tompkins, A.M., Warszawski, L., Wisser, D., Schellnhuber, H.J., 2014. Multisectoral climate impact hotspots in a warming world. Proc. Natl. Acad. Sci. U. S. A. 111, 3233–3238. https://doi.org/10.1073/pnas.1222471110

Quilcaille, Y., Gasser, T., Ciais, P., Boucher, O., 2023a. CMIP6 simulations with the compact Earth system model OSCAR v3.1. Geosci. Model Dev. 16, 1129–1161. https://doi.org/10.5194/gmd-16-1129-2023

Quilcaille, Y., Gudmundsson, L., Beusch, L., Hauser, M., Seneviratne, S.I., 2022. Showcasing MESMER-X: Spatially Resolved Emulation of Annual Maximum Temperatures of Earth System Models. Geophys. Res. Lett. 49, e2022GL099012. https://doi.org/10.1029/2022GL099012

Quilcaille, Y., Gudmundsson, L., Seneviratne, S.I., 2023b. Extending MESMER-X: a spatially resolved Earth system model emulator for fire weather and soil moisture. Earth Syst. Dyn. 14, 1333–1362. https://doi.org/10.5194/esd-14-1333-2023

Riahi, K., Schaeffer, R., Arango, J., Calvin, K., Guivarch, C., Hasegawa, T., Jiang, K., Kriegler, E., Matthews, R., Peters, G.P., Rao, A., Robertson, S., Sebbit, A.M., Steinberger, J., Tavoni, M., Van Vuuren, D.P., 2022. Mitigation pathways compatible with long-term goals. Clim. Change 2022 Mitig. Clim. Change Contrib. Work. Group III Sixth Assess. Rep. Intergov. Panel Clim. Change. https://doi.org/10.1017/9781009157926.005

Rocklin, M., 2015. Dask: Parallel Computation with Blocked algorithms and Task Scheduling. Presented at the Python in Science Conference, Austin, Texas, pp. 126–132. https://doi.org/10.25080/Majora-7b98e3ed-013

Rossum, G. van, Drake, F.L., 2010. The Python language reference, Release 3.0.1 [Repr.]. ed, Python documentation manual / Guido van Rossum; Fred L. Drake [ed.]. Python Software Foundation, Hampton, NH.

Sandstad, M., Aamaas, B., Johansen, A.N., Lund, M.T., Peters, G.P., Samset, B.H., Sanderson, B.M., Skeie, R.B., 2024. CICERO Simple Climate Model (CICERO-SCM v1.1.1) – an improved simple climate model with a parameter calibration tool. Geosci. Model Dev. 17, 6589–6625. https://doi.org/10.5194/gmd-17-6589-2024

Schleussner, C.-F., Ganti, G., Lejeune, Q., Zhu, B., Pfleiderer, P., Prütz, R., Ciais, P., Frölicher, T.L., Fuss, S., Gasser, T., Gidden, M.J., Kropf, C.M., Lacroix, F., Lamboll, R., Martyr, R., Maussion, F., McCaughey, J.W., Meinshausen, M., Mengel, M., Nicholls, Z., Quilcaille, Y., Sanderson, B., Seneviratne, S.I., Sillmann, J., Smith, C.J., Steinert, N.J., Theokritoff, E., Warren, R., Price, J., Rogelj, J., 2024. Overconfidence in climate overshoot. Nature 634, 366–373. https://doi.org/10.1038/s41586-024-08020-9

Schleussner, C.F., Lissner, T.K., Fischer, E.M., Wohland, J., Perrette, M., Golly, A., Rogelj, J., Childers, K., Schewe, J., Frieler, K., Mengel, M., Hare, W., Schaeffer, M., 2016. Differential climate impacts for policy-relevant limits to global warming: The case of 1.5 °c and 2 °c. Earth Syst. Dyn. 7, 327–351. https://doi.org/10.5194/esd-7-327-2016

Schöngart, S., Gudmundsson, L., Hauser, M., Pfleiderer, P., Lejeune, Q., Nath, S., Seneviratne, S.I., Schleußner, C.-F., 2024. Introducing the MESMER-M-TPv0.1.0 module: Spatially Explicit Earth System Model Emulation for Monthly Precipitation and Temperature. EGUsphere 1–51. https://doi.org/10.5194/egusphere-2024-278

Schwaab, J., Hauser, M., Lamboll, R.D., Beusch, L., Gudmundsson, L., Quilcaille, Y., Lejeune, Q., Schöngart, S., Schleussner, C.-F., Nath, S., Rogelj, J., Nicholls, Z., Seneviratne, S.I., 2024. Spatially resolved emulated annual temperature projections for overshoot pathways. Sci. Data 11, 1262. https://doi.org/10.1038/s41597-024-04122-1

Schwind, N., 2025. RIME-X: Emulating regional climate impact distributions using simple climate models and impact models, in: CL3.2.3 – Statistical and Physical Emulators for Climate Impacts. Presented at the EGU General Assembly 2025.

Shiogama, H., Fujimori, S., Hasegawa, T., Hayashi, M., Hirabayashi, Y., Ogura, T., Iizumi, T., Takahashi, K., Takemura, T., 2023. Important distinctiveness of SSP3–7.0 for use in impact assessments. Nat. Clim. Change 13, 1276–1278. https://doi.org/10.1038/s41558-023-01883-2

Smith, C.J., Forster, P.M., Allen, M., Leach, N., Millar, R.J., Passerello, G.A., Regayre, L.A., 2018. FAIR v1.3: a simple emissions-based impulse response and carbon cycle model. Geosci. Model Dev. 11, 2273–2297. https://doi.org/10.5194/gmd-11-2273-2018

team, T. pandas development, 2024. pandas-dev/pandas: Pandas. https://doi.org/10.5281/zenodo.10697587

Tebaldi, C., Snyder, A., Dorheim, K., 2022. STITCHES: creating new scenarios of climate model output by stitching together pieces of existing simulations. Earth Syst. Dyn. 13, 1557–1609. https://doi.org/10.5194/esd-13-1557-2022

Wells, C.D., Jackson, L.S., Maycock, A.C., Forster, P.M., 2023. Understanding pattern scaling errors across a range of emissions pathways. Earth Syst. Dyn. 14, 817–834. https://doi.org/10.5194/esd-14-817-2023

Werning, M., 2024. Gridded maps of global population scaled to match the 2023 Wittgenstein Center (WIC) Population projections. https://doi.org/10.5281/zenodo.13745063

Werning, M., Frank, S., Hooke, D., Nguyen, B., Rafaj, P., Satoh, Y., Wögerer, M., Krey, V., Riahi, K., van Ruivjen, B., Byers, E., 2024a. Climate Solutions Explorer - hazard, impacts and exposure data, v1.0. https://doi.org/10.5281/zenodo.13753537

Werning, M., Hooke, D., Krey, V., Riahi, K., Ruijven, B. van, Byers, E.A., 2024b. Global warming level indicators of climate change and hotspots of exposure. Environ. Res. Clim. 3, 045015. https://doi.org/10.1088/2752-5295/ad8300

Supplementary Information

6 Additional maps of indicators for 2020 and two scenarios in 2050

6.1 Maps of temperature-based climate indicators in 2020 and two scenarios in 2050

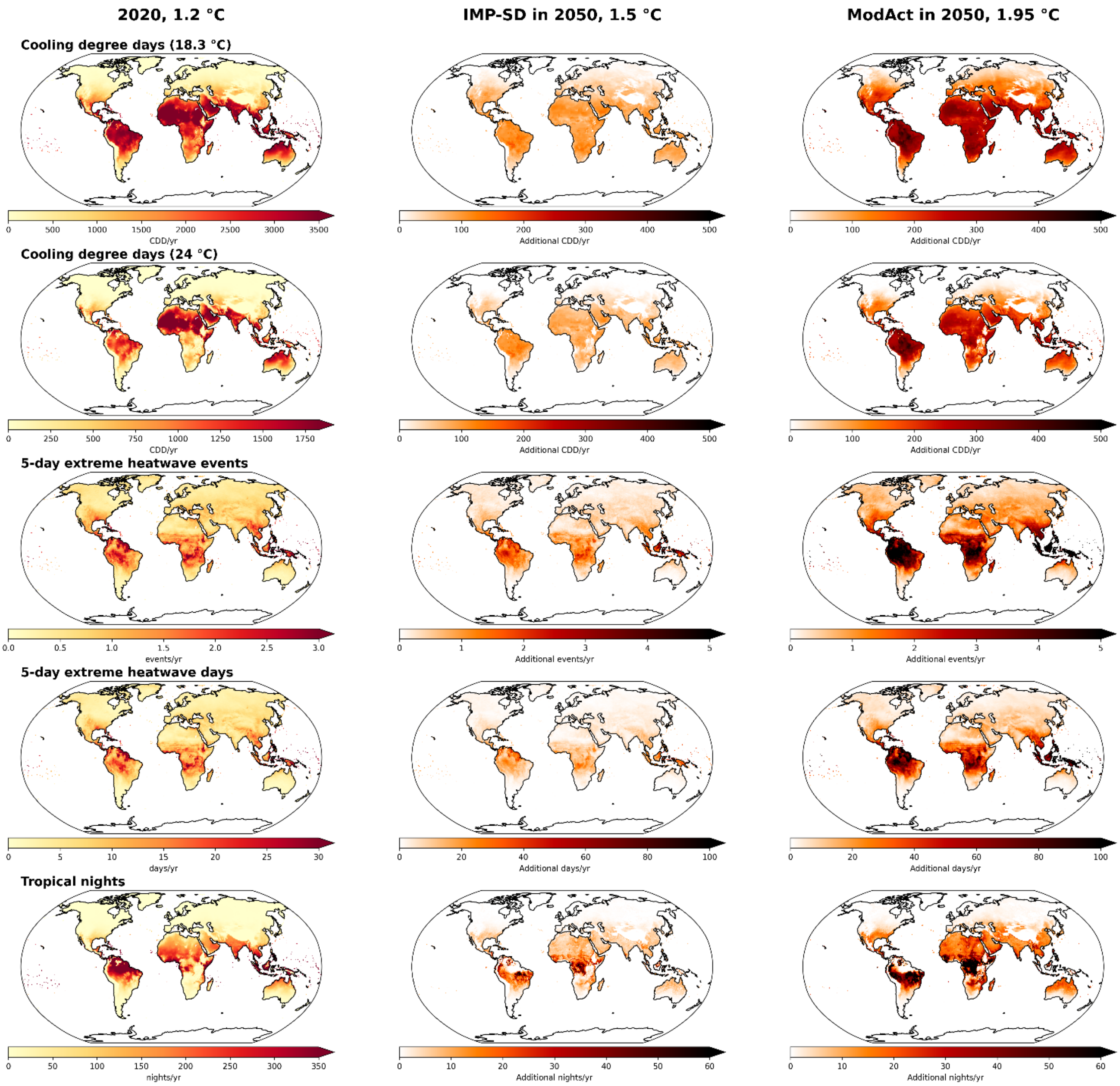

Figure S 1. Global maps of surface air temperature indicators. The indicator maps show the multi model ensemble median values at the respective global warming levels, in 2020 (1.21 °C) and in 2050 for two different scenarios at 1.51 and 1.95 °C. The middle and right columns for 2050 are displayed as % change relative to the 2020 values.

6.2 Maps of water and hydrology-based climate indicators in 2020 and two scenarios in 2050

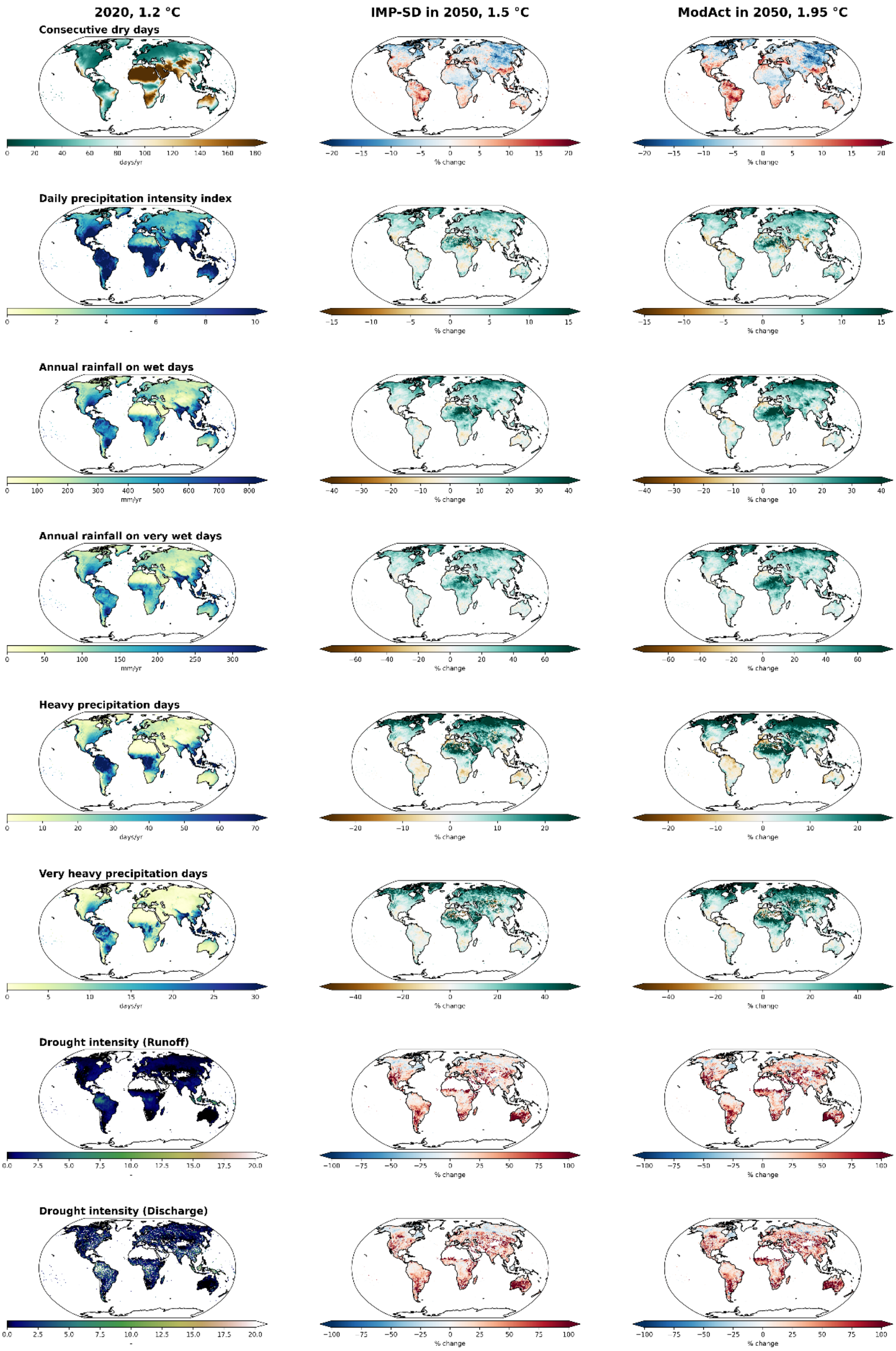

Figure S 2. Global maps of precipitation and hydrological indicators. The indicator maps show the multi model ensemble median values at the respective global warming levels, in 2020 (1.21 °C) and in 2050 for two different

scenarios at 1.51 and 1.95 °C. The middle and right columns for 2050 are displayed as % change relative to the 2020 values. First five rows are precipitation indicators from the Expert Team on Climate Change Detection and Indices (ETCCDI). Bottom two rows for drought intensity derive from hydrological models.

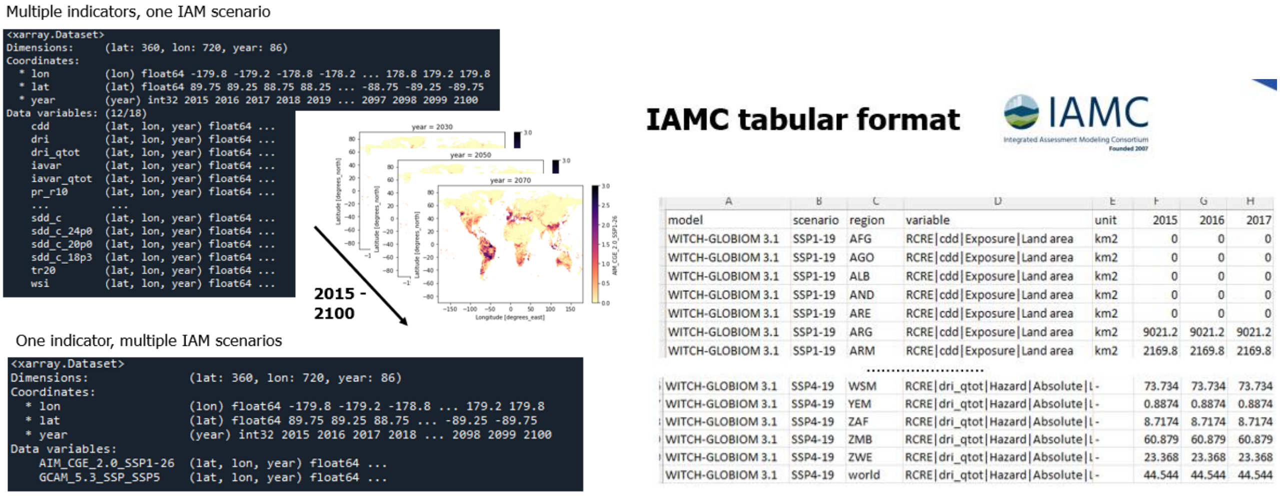

Figure S 3. Example data outputs in gridded netCDF (left) and IAMC template (right) formats. Upper left print view shows an output global gridded netCDF with multiple climate indicators as data variables computed for one GMT pathway through time (2015-2100). Lower left similarly shows an output netCDF but for two GMT pathways as variables for one climate indicator. Right panel shows example IAMC table output for one GMT pathway and multiple climate indicators, aggregated to countries.

7 Evaluating uncertainties

7.1 Regional uncertainties

In order to provide estimates of the regional climate model and scenario uncertainties surrounding the deterministic median estimates provided by RIME, we assess the suitability of using the 5th and 95th percentile temperatures from MAGICC as inputs to RIME to estimate the range of impacts that occur in the input data ensemble. Hence, we compare the 5th and 95th percentiles of:

- The <u>input data ensemble</u>, effectively the "source of truth", comprising the multi-model ensemble from ISIMIP3b for the three available forcing scenarios (SSP1-26, SSP3-70, SSP5-85), with
- The <u>RIME output data, when the 5th and 95th</u> percentile temperatures from MAGICC are used as opposed to the median.

The intention of this experiment aims to evaluate how close the regional ranges of indicators can be estimated using the temperature percentiles, as opposed to using the full multi-model input data ensemble.

For the <u>input data ensemble</u>, all climate model ensemble members contributing to each global warming level are used to calculate the 5th and 95th percentiles. This dataset captures, for a given global warming level, the regional climate model uncertainty (from five GCMs) and separates the climate forcing scenario uncertainty, i.e. for the same GCM, the regional results for a given warming level will vary depending on which SSP-RCP forcing scenario is used.

For the <u>RIME output data</u>, a different process is required. Using all available vetted emissions scenarios from the IPCC WGIII AR6 scenarios database (Byers et al., 2022), the following steps are undertaken to calculate the 5th and 95th percentiles of the RIME output data:

- For each GWL, and emissions scenario, the year at which a certain global warming level is reached for the first time, for example 1.5 °C, is evaluated based on the 50^{th} percentile of the Surface Temperature (GSAT) of the MAGICC runs.
- The year of the first exceedance is then used to look up the corresponding temperature of the 5^{th} and 95^{th} percentile MAGICC timeseries.
- For both the 5^{th} and 95^{th} percentiles, the median value of the temperatures from all emissions scenarios is calculated for each GWL is calculated (Figure S 43a,b).
- The resulting median temperatures for the 5^{th} and 95^{th} percentiles are subsequently run through RIME to obtain the emulated variables.

This analysis could also be done for each climate forcing scenario, which is included in Figure S 3. In this case, the three available climate forcing scenarios (SSP1-26, SSP3-70, SSP5-85) are allocated matching scenario categories (Table S1, Kikstra et al., 2022; Riahi et al., 2022) in order to not use data from forcing scenarios that are substantially different to the scenario being emulated.

Table S 1. To calculate the change between the median GSAT and either the 5^{th} or 95^{th} percentile, for each climate forcing scenario (left column), the median GSAT of all scenarios in the respective Categories (right column) was calculated.

Climate forcing scenario from the input data ensemble	Respective climate “Category(ies)” for comparison from the IPCC WGIII AR6 scenarios database (Riahi et al., 2022)
SSP1-26	C1: limit warming to 1.5°C (>50%) with no or limited overshoot
	C2: return warming to 1.5°C (>50%) after a high overshoot
	C3: limit warming to 2°C (>67%)
SSP3-70	C7: limit warming to 4°C (>50%)
SSP5-85	C8: exceed warming of 4°C (≥50%)

It is noted that the allocation of scenario categories to climate forcing scenarios is not perfect, but the intention is to capture the median difference across forcing scenarios between the 50^{th} percentile and the 5^{th} and 95^{th} percentile of the GSAT of the MAGICC runs as illustrated by the boxplots in Figure S 3a and b. Whilst many emissions scenarios can be assessed at the same median global warming level, the distribution of GSAT uncertainty around each scenario differs, primarily due to differing compositions and emission rates of GHGs in the scenarios (as shown by the temperature difference between the 5^{th} and 95^{th} percentiles in Figure S 3c).

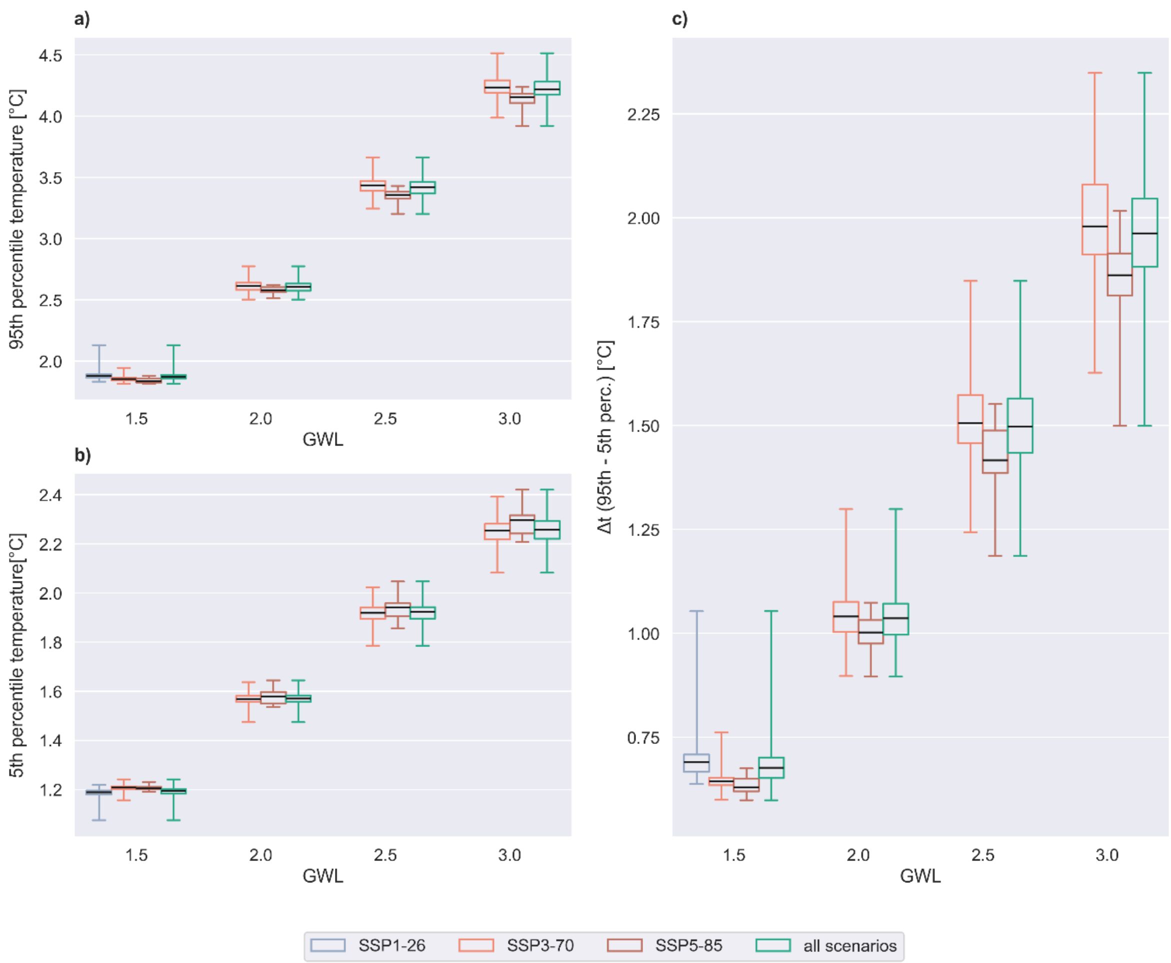

Figure S 4. The figure shows the median global warming level (GWL) on the x-axis, and the 5th and 95th percentile GSATs from MAGICC on the y-axis (panels a and b) for all emissions scenarios in green, as well as per climate forcing scenarios. In the assessment of regional uncertainties, the median percentile values across all scenarios is used. Panel c shows the difference between the 95th and 5th percentiles, calculated for each scenario. It is not used in subsequent calculations but shown for information only.

Using the method described above, the uncertainty range of the input data ensemble and the RIME output as expressed by the 5th and 95th percentiles can then be compared. In Table S2, this comparison is shown for the indicator ‘Cooling degree days (24 °C)’ and the R10 regions. The comparison of the median is omitted as in this case RIME outputs the exact values.

Table S 2. Median value and % difference of RIME to the GCM ensemble for the indicator ‘Cooling degree days (24 °C)’ at GWLs 1.5 °C, 2.0 °C, 2.5 °C, and 3.0 °C

		1.5 °C			**2.0 °C**			**2.5 °C**			**3.0 °C**		
			% difference of RIME to the GCM ensemble			**% difference of RIME to the GCM ensemble**			**% difference of RIME to the GCM ensemble**			**% difference of RIME to the GCM ensemble**	
Region	**Unit**	**RIME**	p5	p95	**RIME**	p5	p95	RIME	p5	p95	RIME	p5	p95

Latin America and the Caribbean	days yr^{-1}	746	4	1	890	-2	12	1069	-5	14	1193	-5	-2
South Asia	days yr^{-1}	1094	3	4	1213	-4	7	1332	-7	10	1446	-9	0
Sub-Saharan Africa	days yr^{-1}	1099	4	2	1251	-3	8	1398	-5	9	1554	-7	-2
Centrally planned Asia	days yr^{-1}	156	18	7	185	7	18	223	0	25	256	-5	7
Middle East	days yr^{-1}	1269	6	2	1397	0	7	1536	-3	12	1699	-6	3
Eastern and Western Europe	days yr^{-1}	63	12	9	85	-1	28	111	-7	36	143	-15	8
North America	days yr^{-1}	90	16	9	110	12	16	129	8	25	151	0	7
Other countries of Asia	days yr^{-1}	933	3	3	1067	-3	11	1212	-5	17	1359	-7	5
Pacific OECD	days yr^{-1}	787	4	0	872	0	8	977	-3	13	1099	-5	2
Reforming Economies of Eastern Europe and the Former Soviet Union	days yr^{-1}	62	6	-2	77	-4	19	100	-9	23	124	-9	2

The same comparison of the percentiles between the input data ensemble and the RIME output data can also be made for one region and multiple indicators (Table S3). Note that for the hydrology indicators, the 95th

percentile values for the GWLs 2.5 °C and 3.0 °C are missing, as the corresponding 95th percentile temperatures are above 3.0 °C, which is the maximum global warming level for these indicators (Werning et al., 2024b).

Table S 3. Median value and % difference of RIME to the GCM ensemble for selected indicators and the region 'Countries of centrally planned Asia' at the GWLs 1.5 °C, 2.0 °C, 2.5 °C, and 3.0 °C

		1.5 °C			2.0 °C			2.5 °C			3.0 °C		
			% difference of RIME to the GCM ensemble			**% difference of RIME to the GCM ensemble**			**% difference of RIME to the GCM ensemble**		**% difference of RIME to the GCM ensemble**		
Indicator	Unit	**RIME**	p5	p95	**RIME**	p5	p95	**RIME**	p5	p95	**RIME**	p5	p95
Consecutive dry days	days yr^{-1}	96	5	-4	94	7	-8	90	7	-8	88	8	-
Heatwave events (5 days, 99th perc.)	events yr^{-1}	1	60	13	2	35	16	3	18	5	3	12	-
Heatwave days (5 days, 99th perc.)	days yr^{-1}	12	57	24	22	32	40	32	18	46	43	7	-
Very heavy precipitation days	days yr^{-1}	6	16	-7	6	18	-1	7	19	0	7	22	-
Very wet days	days yr^{-1}	305	4	-7	314	4	-2	335	5	0	350	8	-
Simple precipitation intensity index	-	6	6	-3	6	6	-1	7	7	1	7	8	-
Cooling degree days (24.0 °C)	days yr^{-1}	156	18	7	185	7	18	223	0	25	256	--5	-
Tropical nights	days yr^{-1}	24	-3	3	28	-8	14	32	-10	22	36	-12	-

7.2 Trend analysis using Pearson correlation coefficient

The Pearson correlation is chosen to analyse if the timeseries across all global warming levels (GWLs) has a positive or negative trend, either on a country/region or grid cell level. A p value of $p < 0.05$ is used to test for statistical significance and a correlation coefficient of $r \geq 0.8$ and $r \leq -0.8$ is chosen as the thresholds for a positive or negative trend, respectively. It should be noted that small sample sizes can affect the statistical power of the correlation. While we are of the opinion that the analysis using a Pearson correlation with the parameters described above provides a robust estimate of the trend in the timeseries, the option to test for strict monotony is also included in the package.

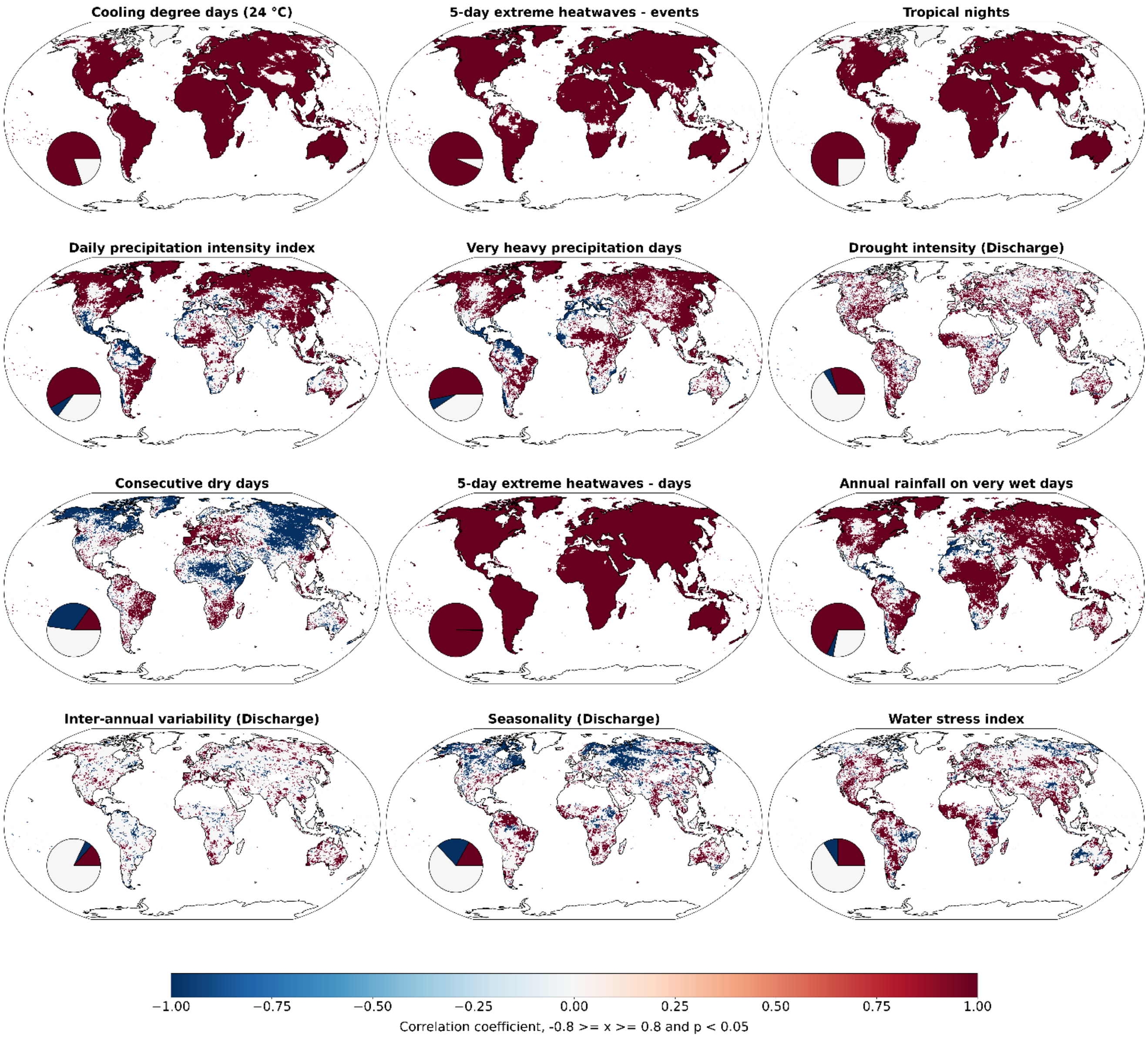

Figure S 5. Pearson correlation coefficient for every grid cell. Shown are only correlation coefficients -0.8 >= x >= 0.8 and with a p value < 0.05. The pie charts in the bottom left corner show the percentage of pixel with a positive trend (x ≥ 0.8 and p < 0.05) in red, the percentage of pixels with a negative trend in blue (x ≤ -0.8 and p < 0.05), and the percentage of pixels with no trend in white.

7.3 Decomposition of uncertainties

To demonstrate versatility of the framework, uncertainties in the population exposure to climate impacts across the emissions scenarios, MAGICC GSAT percentiles, and socioeconomic scenario, are assessed through time, using an approach similar to the one used by Lehner and Deser (2023) and Hawkins and Sutton (2009). All 245 possible combinations of emissions scenarios (7), socioeconomic scenarios (5) and MAGICC warming percentiles (7) are run through RIME (Table S 4). From the RIME output, the total exposed population is used and a 4^{th}-order polynomial is fitted to each of the 245 time series. To calculate the emissions scenarios uncertainty, the 35 available time series (product of 5 socioeconomic scenarios and 7 MAGICC percentiles) for each emissions scenario are averaged and subsequently the variance of the seven means is calculated. The same is done also for both the socioeconomic scenarios and the MAGICC percentiles. Finally, the variances are summed and the relative contribution of each category is calculated.

Changes in uncertainty are illustrated for six key indicators and two regions, Europe and sub-Saharan Africa (Figure S 6, Figure S 7). In Europe, climate uncertainty dominates initially, followed by emissions scenario uncertainty. Socioeconomic plays a minor role in the exposure because the differences in SSP scenarios are comparably small. In sub-Saharan Africa, the differences in socioeconomic scenario dominate through the century, given that there are large differences in total population between the SSP scenarios, driven by widely varying levels of fertility.

Table S 4: Selection of emissions scenarios, socioeconomic scenarios and MAGICC percentiles used for the decomposition of uncertainty.

Emissions scenario uncertainty (7)		
Model, Scenario	*Note*	*Comments*
REMIND-MagPIE 2.1-4.2, SusDev_SDP-PKBudg1000	IPCC AR6 WGIII IMP-SP “Shifting Pathways”	Seven high quality emissions scenarios prominent in the IPCC spanning a range of potential temperature outcomes. All data sourced from the AR6 Scenarios Database (Byers et al., 2022)
MESSAGEix-GLOBIOM-GEI 1.0, SSP2_openres_lc_50	IPCC AR6 WGII IMPRen “Renewables”	
IMAGE 3.0.1, SSP1-19	SSP1 marker	
IMAGE 3.0.1, SSP1-26	SSP1 marker	
WITCH 5.0, CO_Bridge	IPCC AR6 WGII IMP-GS “Gradual Strengthening”	
MESSAGE-GLOBIOM 1.0, SSP2-45	SSP2 marker	
IMAGE 3.0, EN_INDCi2030_3000f	IPCC AR6 WGII IMP-ModAct “Moderate Action”	
Global climate response uncertainty (MAGICC percentiles) (7)		
5.0, 16.7, 33.0, 50.0, 67.0, 83.3, 95.0		The seven percentiles of climate warming uncertainty reported by MAGICC for each emissions scenario

	from the AR6 Scenarios Database (Byers et al., 2022)
Socioeconomic uncertainty in population growth and distribution (5)	
SSP1, SSP2, SSP3, SSP4, SSSP5	The five projections of population growth and distribution, based on the updated projections from (KC et al., 2024; Werning, 2024).

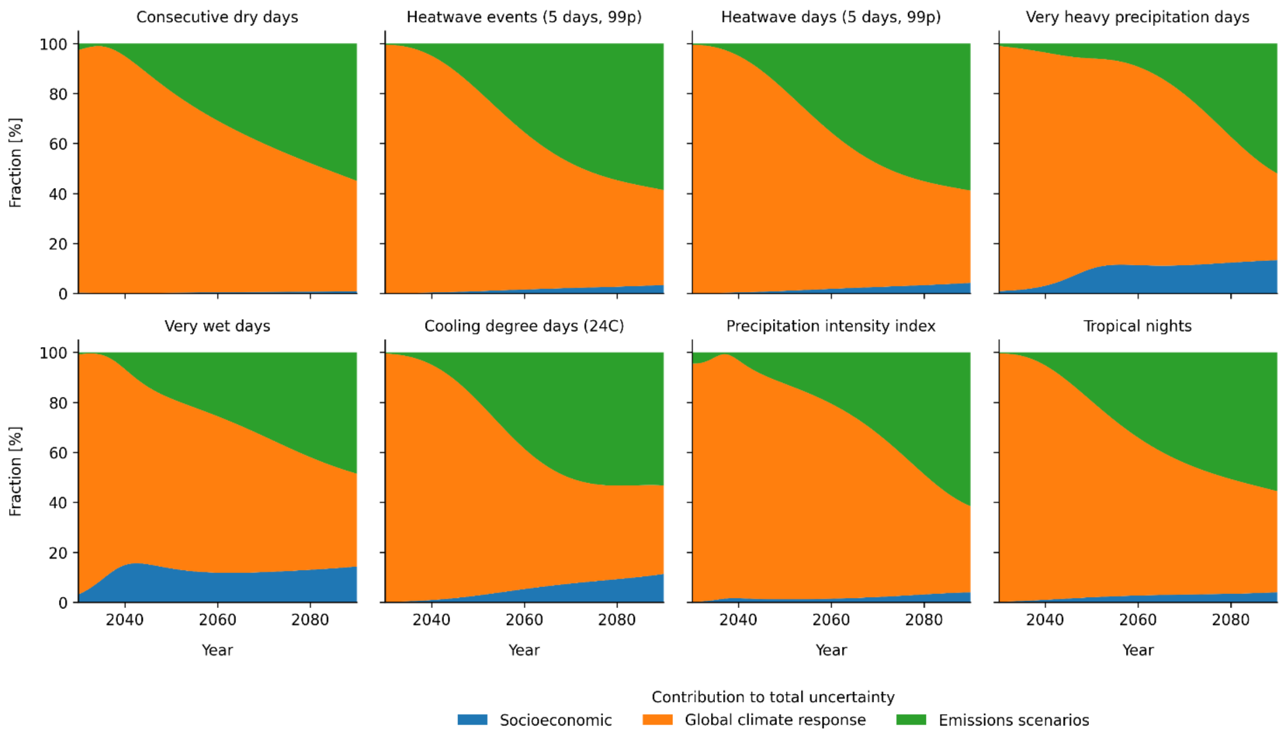

Figure S 6: Relative contribution of different sources of uncertainty for the exposed population in the European Union and a selection of indicators.

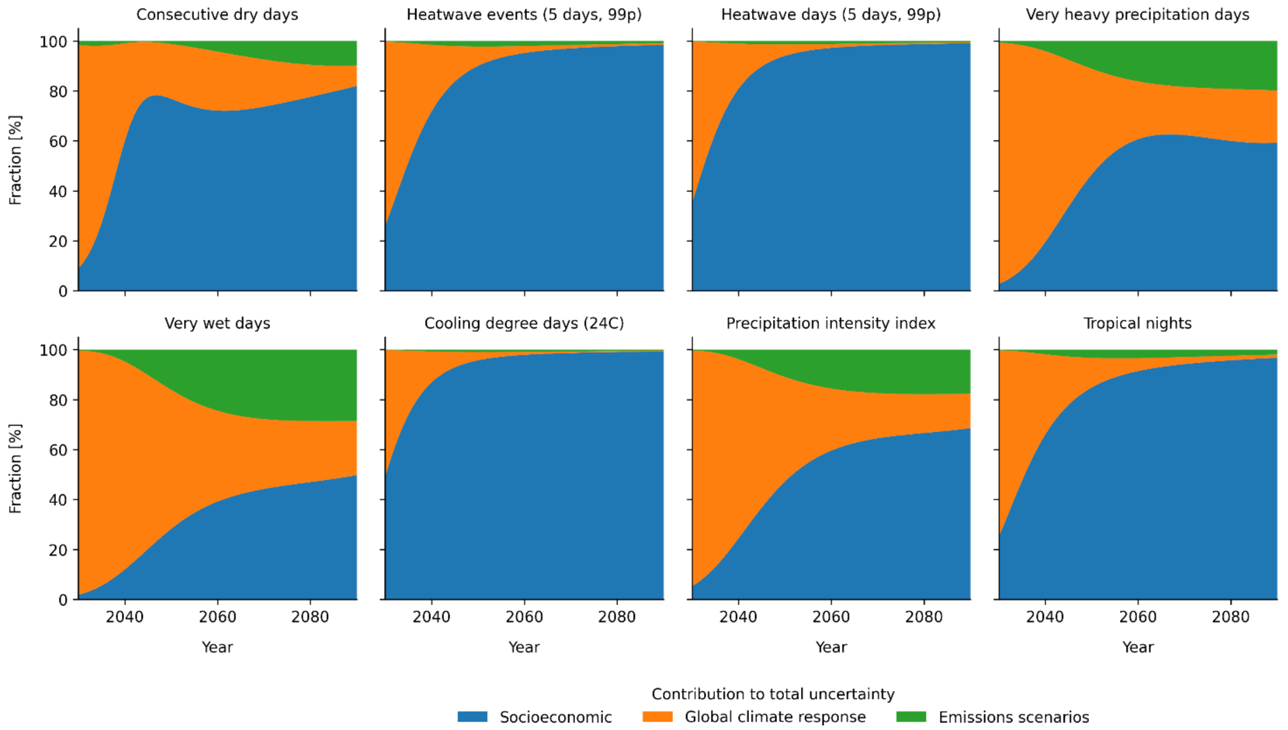

712

713 *Figure S 7: Relative contribution of different sources of uncertainty for the exposed population in Sub-Saharan Africa*
714 *and a selection of indicators.*

715